Nanocomposite Fe1xO=Fe3O4, Fe=Fe1xO thin films prepared by RF sputtering and revealed by magnetic coupling effects

Bruno Mauvernay, Lionel Presmanes, Corine Bonningue, Philippe Tailhades

Nanocomposite $Fe_{1-x}O/Fe_3O_4$, $Fe/Fe_{1-x}O$ thin films prepared by RF sputtering and revealed by magnetic coupling effects

B. Mauvernay, L. Presmanes*, C. Bonningue, Ph. Tailhades

CIRIMAT, UMR CNRS 5085, Université Paul Sabatier, 118 Route de Narbonne, 31062 Toulouse Cedex 9, France

Abstract

Magnetic and semi-conducting nanocomposite iron oxide thin films have been prepared under bias polarization, by radio-frequency sputtering of a magnetite target. The nature of the phases obtained in the thin films depends on the bias power density. The increase in power density, from 0 to 110 mW/cm^2, allows the preparation of magnetite, magnetite/wustite and wustite/α-iron nanocomposites successively. Magnetic measurements at low temperature show exchange bias for two-phases films even though the minor phase is not detected by grazing angle X-ray diffraction. The exchange bias can reach very high values of about 4300 Oe. Electrical properties at room temperature are interpreted taking into account both the modifications of the film compactness, and the nature of the phases from which they are made.

Keywords: Iron oxides; Magnetic coupling; Exchange bias; Sputtering; Nanocomposite; Magnetite; Wustite

1. Introduction

The preparation of iron oxide thin films can lead to devices with attractive optical, magnetic, and semi-conducting properties, which can be tailored by altering the preparation parameters. Among all the vacuum processes used for producing films, the sputtering process is one of the most popular. It allows preparation of film at moderate temperatures, making deposition possible on various substrates with high homogeneity and good uniformity. As a consequence, the sputtering technique is widely used in research laboratories as well as in industrial production units. But, the attractiveness of RF sputtering is also that it offers the possibility of preparing materials, especially oxides, which can be out-of-equilibrium or non-stoichiometric at room temperature (RT).

During sputtering of an oxide target, the layer grown on the substrate is submitted to continuous bombardment with high energy species from plasma and target, which can induce specific characteristics or properties [1–3]. In this study, we tuned bias sputtering conditions to obtain nanocomposite iron oxide from a magnetite target. With bias sputtering, the growing layer is submitted to a strong Ar^+ bombardment and leads to the formation of reduced thin films by impoverishment of the oxygen content in the growing layer.

Because of its great sensitivity, magnetic measurement, is particularly suited for determining the presence of phases with different magnetic properties. After field cooling and below the Néel temperature ($T_{Néel}$), the hysteresis loop of materials made of both antiferromagnetic (AFM) and ferromagnetic (FM) or antiferromagnetic and ferrimagnetic (FI) phases, is for instance shifted along the negative field axis. This loop shift is known as exchange bias (He) [4–8]. The measurement of the exchange bias parameter is particularly suitable to study nanocomposites made of AFM/FM or AFM/FI phases which are often difficult to reveal by X-ray or electron diffraction. In this report, magnetic measurements are used to study the influence of substrate polarization on phase formation and the occurrence of nanocomposites in thin films made of iron and oxygen. The resulting changes in the semi-conducting properties of such films are also studied.

*Corresponding author. Tel.: +33 5 61 55 81 03; fax: +33 5 61 55 61 63.
E-mail address: presmane@chimie.ups-tlse.fr (L. Presmanes).

doi:10.1016/j.jmmm.2007.05.042

2. Experimental

Iron oxide thin films were prepared by RF magnetron sputtering using a Fe_3O_4 ceramic target containing 5% of FeO. The apparatus is an Alcatel SCM-400 equipped with an RF-generator (13.56 MHz), and a pumping system composed of a mechanical pump coupled with a diffusion pump. A residual vacuum of 10^{-5} Pa was reached in the sputtering chamber before introducing the argon gas. The films were deposited on glass slides under pure argon gas flow and the working pressure was kept at a value of 0.5 Pa. The distance between the target and the substrates was 70 mm and the power density applied to the magnetite target was 860 mW/cm^2. Different RF bias power densities from 0 to 110 mW/cm^2 were also applied to the substrate. The conditions of deposition are summarized in Table 1.

Film thickness was measured using a Dektak 3030ST profilometer. Structural characterizations of the films were performed by grazing angle X-ray diffraction (XRD) ($\alpha = 1^\circ$) on a Siemens D5000 diffractometer. The morphology and microstructure of the as-deposited samples were examined by scanning electron microscopy (SEM) performed on a JEOL JSM 6700F system. The resistivity was determined on the as-deposited samples with a QuadPro four-point probe device from Signatone, equipped with a Keithley SMU 237. Magnetic measurements were done at 5 K with a superconducting quantum interference device (SQUID) magnetometer MPMS quantum design 5.5, on samples deposited on both sides of a thin (0.1 mm) glass substrate.

3. Results and discussion

3.1. Preparation

Nanocomposite iron oxide thin films were deposited with variable bias applied during film growth. Fig. 1 shows that the deposition rate was affected by the substrate bias. When the RF bias applied to the substrate was changed from 0 to 110 W/cm^2, the deposition rate decreased linearly from 5.1 to 1.8 nm/mn. The deposition rate is due to sputtering from the accelerated Ar^+ ions at the surface of the growing film.

Fig. 2 shows XRD patterns of the biased and unbiased thin films. When no bias was applied to the growing film, the XRD pattern of the material obtained showed a pure Fe_3O_4 iron oxide with a well-defined spinel structure. The microstructure of such thin films is presented in Fig. 3a and shows a columnar structure. This type of structure is characteristic of sputtered thin films in diode configuration.

When the substrate was biased with 6 mW/cm^2, the XRD pattern of the thin film showed that all diffraction peaks of the spinel structure were shifted to lower angles. This shift signifies in-plane compression stress [9,10]. The shift and the broadening of diffraction patterns leading to a possible partial overlap of the spinel and wustite phase peaks made a clear identification of the crystalline phases impossible using only XRD.

For samples polarized with power densities lying between 16 and 63 mW/cm^2, XRD only revealed a NaCl-type diffraction pattern (Fig. 1) due to the $Fe_{1-x}O$ wustite phase. As the film grows, oxygen loss is caused by the strong bombardment by high-energy incident Ar^+ cations. Thus, the applied bias gradually led to the formation of a $Fe_{1-x}O$ phase. Fig. 3b shows a SEM image of a thin film prepared with a bias power density of 32 mW/cm^2. This image shows that bias sputtering tends to improve film densification and smoothness. As shown before [1,11], the average roughness R_a can be decreased by about 70–80% when the substrate is exposed to bias during the deposition process.

Finally, for the highest polarizations applied to the substrates (up to 80 mW/cm^2), α-Fe mixed with $Fe_{1-x}O$ iron oxide was formed. The SEM image (Fig. 3c) of thin film deposited with 80 mW/cm^2 again shows high densification of the thin film. We were unable to observe α-Fe nano-metallic particles by SEM.

According to the XRD patterns it is clear that the stoichiometry of the thin film can be controlled, simply by adjusting the bias power. The substrate bias acts as a key parameter to move through the Fe–O phase diagram from magnetite (Fe_3O_4) to reduced phases such as wustite ($Fe_{1-x}O$) and even metallic iron (α-Fe).

Table 1
Sputtering parameters

				Magnetron configuration			
Target (wt%)				95% Fe_3O_4–5% FeO			
Gas pressure (Pa)				0.5			
Target–substrate distance (mm)				70			
Film thickness (nm)				300			
RF power density (mW/cm^2)				860			
Bias power density (mW/cm^2)	0	16	32	48	63	80	110
Deposition rate (nm/mn)	5.2	4.2	4.0	3.5	3.0	2.8	1.8
Deposition temperature				Water cooling			
Substrate				Glass slide			

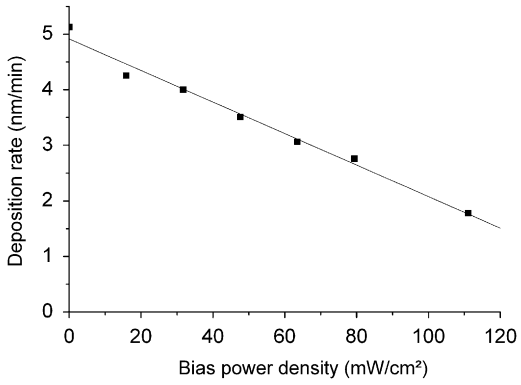

Fig. 1. Deposition rate versus the applied RF bias power density.

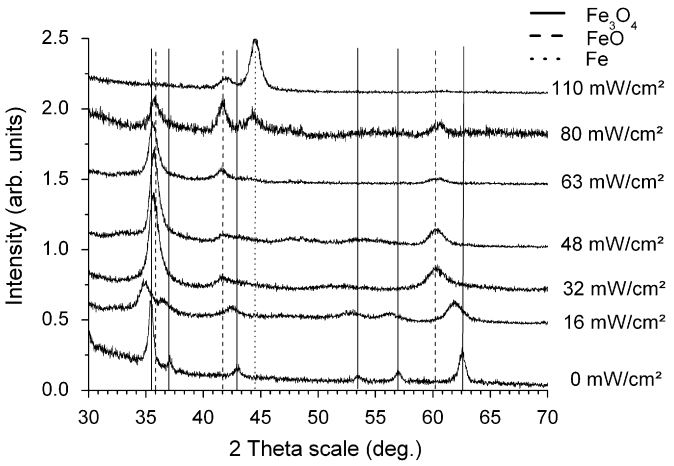

Fig. 2. X-ray diffraction patterns for 300 nm thin films deposited with different bias power densities.

3.2. Electric properties

Fig. 4 shows the electrical resistivity of "as-deposited" thin films versus the applied RF bias power density at RT. The evolution of the resistivity can be described in three stages. First, it decreases from 0.28 to 0.03 Ω cm as bias power density increased from 0 to 16 mW/cm^2. This can be ascribed to the resulting strong densification due to bias (Fig. 3b).

The steep increase in resistivity at the second stage can be attributed to an increase of wustite proportion in the film, as revealed by XRD measurements. In fact, wustite is more resistive than magnetite [12].

Finally, for samples prepared with a bias power density of 63 mW/cm^2, a decrease in resistivity was observed. At this stage, this could not be explained by the XRD results, because only one wustite phase is crystallized. Nevertheless, the resistivity of the thin films continues to fall for the highest bias power densities. As shown previously, metallic iron was formed for such very energetic preparation conditions. The decrease in resistivity observed above about 50 mW/cm^2 can then be attributed to the formation of α-Fe precipitated in the $Fe_{1-x}O$ matrix. For the highest polarization (111 mW/cm^2) the thin film resistivity is very

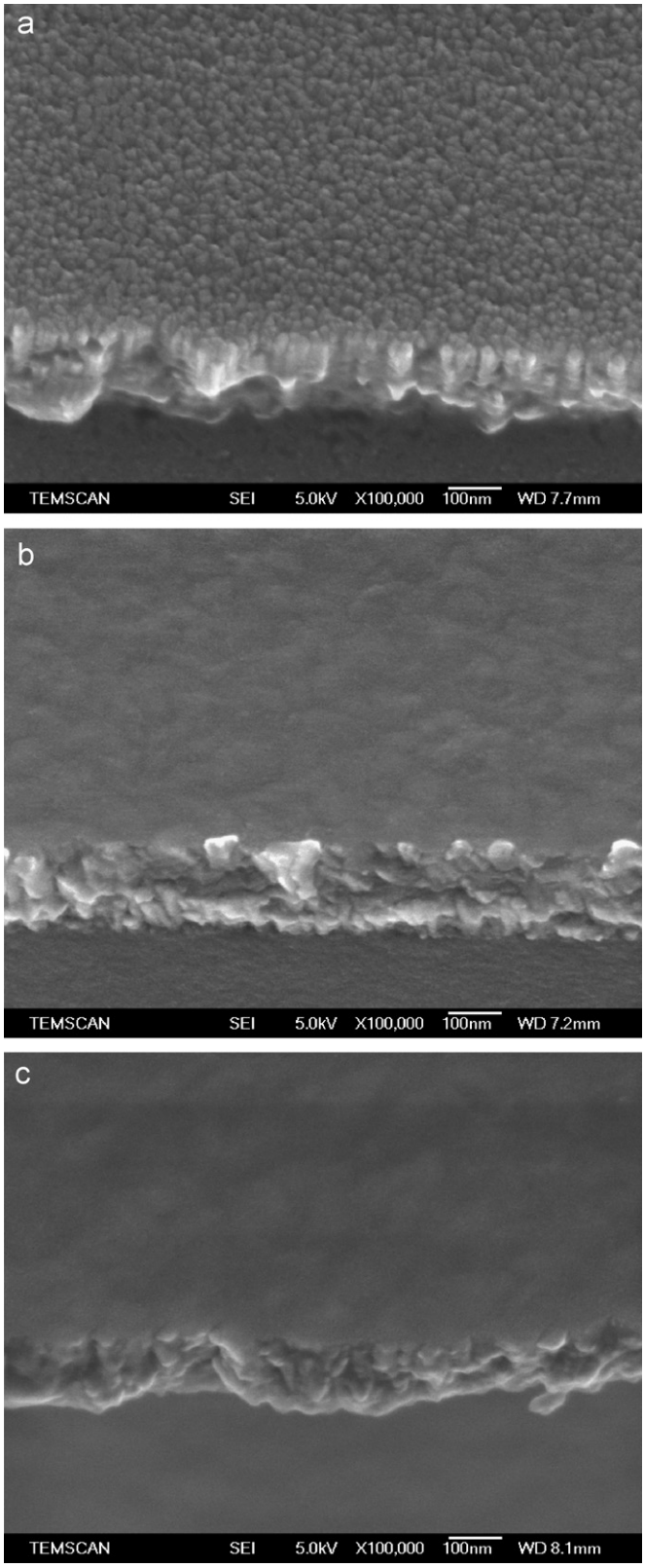

Fig. 3. SEM images (×100 000) of thin films deposited with different bias power densities: (a) 0 mW/cm^2, (b) 32 mW/cm^2, and (c) 80 mW/cm^2.

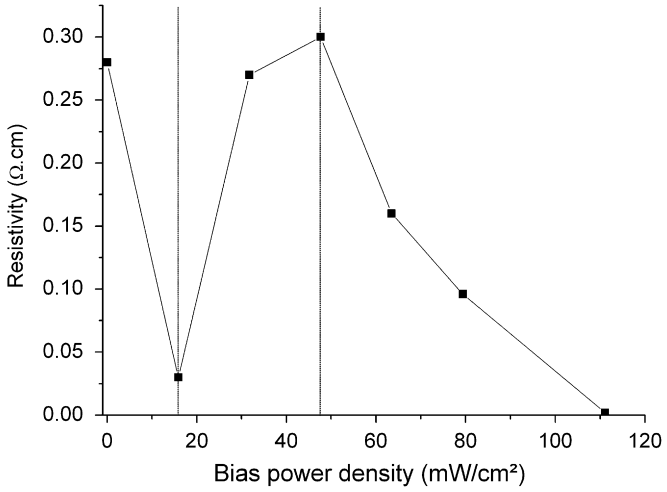

Fig. 4. Electrical resistivity of "as-deposited" thin films versus the applied RF bias power density.

low and close to 0.002 Ω cm, because the deposited material is mainly made of metallic iron.

3.3. Magnetic properties

Fig. 5 shows the hysteresis loops of magnetization versus magnetic field at 5 K, for thin films prepared without any bias (Fig. 5a) or with 32 and 111 mW/cm^2 (Fig. 5b and c) bias power density, respectively. These curves were obtained after cooling from RT to 5 K under a 40 kOe magnetic field. Fig. 5 shows some modifications in hysteresis curve shape and amplitude, due to the sample polarization. In particular, important changes in saturation magnetization (Ms) and exchange bias (He) are observed. Fig. 6 shows the evolution of Ms and He at 5 K versus the applied bias power densities. The exchange bias parameter quantifies the coupling effect and is defined by $He = -(H_{right} + H_{left})/2$; H_{right} and H_{left} being the points where the loop intersects the axis of the applied field.

First of all, when zero bias power density was applied to the substrate, for a pure spinel phase (according to the XRD diagram shown in Fig. 2), the saturation magnetization is close to 330 emu/cm^3. This value is lower than that of bulk magnetite (~480 emu/cm^3). This difference can be attributed to the compactness of the thin film, which is not equal to 1 as showed in Fig. 3a. On the other hand, it could be due to the presence of a small amount of wustite. Careful study of the sputtering ceramic target revealed that it contains about 5% weight wustite. This percentage was determined by thermogravimetric analysis on part of the target ground to powder. The film could then contain at least 5% of wustite which is AFM at 5 K ($T_{Néel} = 198$ K). This hypothesis is confirmed by the measurement of a small exchange bias (He = 13 Oe), corresponding to a coupling effect between a FI phase (Fe_3O_4) and an AFM phase ($Fe_{1-x}O$).

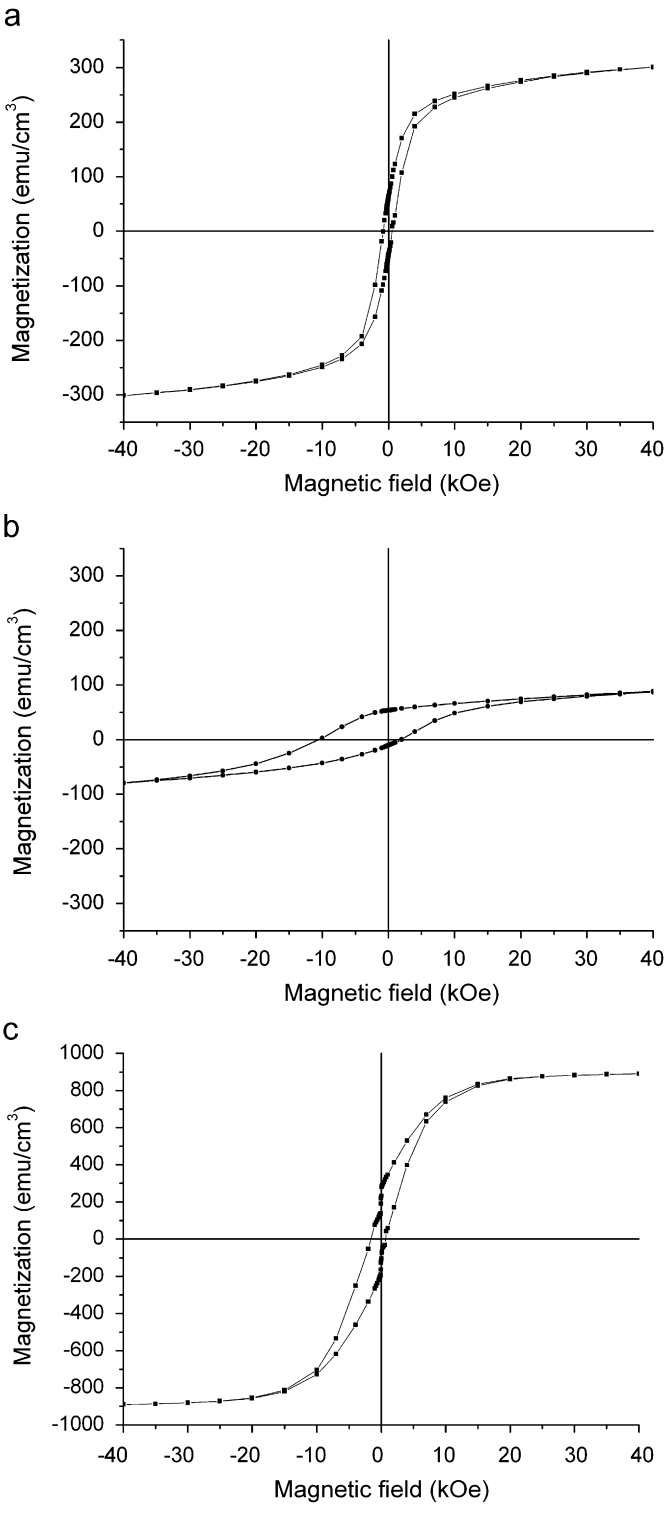

Fig. 5. Magnetization loops of thin films (300 nm on each side) at 5 K deposited with different bias power densities: (a) 0 mW/cm^2, (b) 32 mW/cm^2, and (c) 111 mW/cm^2.

The slight increase in saturation magnetization (350 emu/cm^3) for the sample prepared with a bias power density of 16 mW/cm^2 can be attributed to film densification. However, the theoretical Ms value of magnetite cannot be reached because of the simultaneous creation of

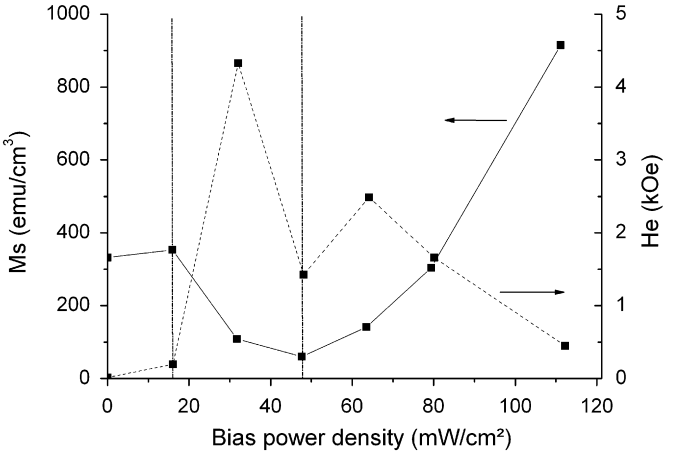

Fig. 6. Evolution of magnetization at saturation (Ms) and the exchange bias (He) at 5 K versus the applied RF bias power density.

wustite, which is revealed by the increase in He. As described before, grazing angle XRD was not able to identify the wustite phase in this sample, but thanks to magnetic measurement and coupling effect, this reduced phase was highlighted.

The steep decrease in saturation magnetization for samples prepared with 32 and 48 mW/cm^2 bias power densities is attributed to the massive precipitation of wustite, as shown in Fig. 2.

A very strong exchange bias (4.3 kOe) is observed for the sample prepared at 32 mW/cm^2. For this value of bias power density, the ratio between Fe_3O_4 and $Fe_{1-x}O$ seems to be close to an optimal value to make a strong coupling effect. Fig. 5b shows the hysteresis loop of this sample. The shift to negative field and the decrease in saturation magnetization are clearly observed.

When the bias power density was increased to 48 mW/cm^2, the proportion of FM phase became lower and He decreased to 1.5 kOe. As explained before, for 63 mW/cm^2 the presence of metallic iron is assumed because of the decrease in RT resistivity. This hypothesis is confirmed by the increase in saturation magnetization from 60 to 140 emu/cm^3. The simultaneous increase in exchange bias up to 2.5 kOe could then be attributed to a coupling effect between a FM phase (α-Fe) and an AFM phase $Fe_{1-x}O$). If Fe_3O_4 was still present in this thin film, a shift in the magnetization loop, because of the coupling effect FM/FI, like in the $CoFe_2/CoFe_2O_4$ system [13,14], would have to appear and to remain even at temperatures well above the Néel temperature of wustite (198 K). However, this shift was not observed at 300 K, showing that there is no FI phase allowing magnetic coupling with the FM phase. The spinel phase then seems to be completely reduced in $Fe_{1-x}O$ and/or α-Fe due to the high-energy conditions of bombardment.

Finally when the value of the bias power density was above 63 mW/cm^2, the amount of metallic iron tended to be very high, leading to a strong increase in saturation magnetization. The value of Ms is close to 300 emu/cm^3 for a bias of 80 mW/cm^2 and reaches 915 emu/cm^3 for the highest value (111 mW/cm^2) as shown in Figs. 5c and 6. Simultaneous decrease of the coupling effect above 63 mW/cm^2 is due to the prominence of only one phase (α-Fe).

4. Conclusion

Bias sputtering is generally used to improve the microstructure of thin films prepared by sputtering. In this paper we showed that this easy-to-control process can generate strongly reducing conditions during deposition of thin films and lead to the preparation of different iron oxides nanocomposites. The nanocomposites (oxide–oxide or metal–oxide) obtained by applying a bias to the substrate were mainly revealed by magnetic coupling effects. For specific preparation conditions, a maximum value of exchange bias (4.3 kOe) was reached. Thus, sputtering appears not only to be a simple physical way to prepare thin films, but also to act like a chemical reactor in which the intensity of reduction reactions can easily be managed by fine-tuning the bias power density.

This promising process allows, from the present moment in time, the preparation of out-of-equilibrium oxides or compounds (oxide–oxide, metal–oxide) at moderate temperatures, which are worth for further physico-chemical studies. Especially magneto-transport properties below the Néel temperature of $Fe_{1-x}O$ and catalysis properties would have to be studied carefully.

References

[1] B. Mauvernay, L. Presmanes, S. Capdeville, V.G. de Resende, E. De Grave, C. Bonningue, P. Tailhades, Thin Solid Films 515 (2007) 6532.
[2] E. Mugnier, I. Pasquet, A. Barnabe, L. Presmanes, C. Bonningue, P. Tailhades, Thin Solid Films 493 (2005) 49.
[3] S. Capdeville, P. Alphonse, C. Bonningue, L. Presmanes, P. Tailhades, J. Appl. Phys. 96 (2004) 6142.
[4] S.K. Arora, R.G.S. Sofin, A. Nolan, I.V. Shvets, J. Magn. Magn. Mater. 286 (2005) 463.
[5] J. Nogues, I.K. Schuller, J. Magn. Magn. Mater. 192 (1999) 203.
[6] L.D. Bianco, D. Fiorani, A.M. Testa, E. Bonetti, J. Magn. Magn. Mater. 290–291 (2005) 102.
[7] D. Fiorani, L. Del Bianco, A.M. Testa, K.N. Trohidou, Phys. Rev. B 73 (2006) 092403.
[8] J. Nogues, J. Sort, V. Langlais, V. Skumryev, S. Surinach, J.S. Munoz, M.D. Baro, Phys. Rep. 422 (2005) 65.
[9] T.J. Vink, W. Walrave, J.L.C. Daams, A.G. Dirks, M.A.J. Somers, K.J.A. van den Aker, J. Appl. Phys. 74 (1993) 988.
[10] F. Medjani, R. Sanjines, G. Allidi, A. Karimi, Thin Solid Films 515 (2006) 260.
[11] Y. Peng, C. Park, D.E. Laughlin, J. Appl. Phys. 93 (2003) 7957.
[12] J.-C. Park, D. Kim, C.-S. Lee, D.-K. Kim, Bull. Korean Chem. Soc. 20 (1999) 1005.
[13] N. Viart, R. Sayed Hassan, J.L. Loison, G. Versini, F. Huber, P. Panissod, C. Meny, G. Pourroy, J. Magn. Magn. Mater. 279 (2004) 21.
[14] N. Viart, R.S. Hassan, C. Meny, P. Panissod, C. Ulhaq-Bouillet, J.L. Loison, G. Versini, F. Huber, G. Pourroy, Appl. Phys. Lett. 86 (2005) 192514.